

## Relationship between the Ratio of Ligand to Metal and the Coordinating Ability of Anions. Synthesis and Structural Properties of AgX-Bearing Bis(4-pyridyl)dimethylsilane ( $X^- = \text{NO}_2^-, \text{NO}_3^-, \text{CF}_3\text{SO}_3^-, \text{and PF}_6^-$ )

Jung Woon Lee,<sup>†</sup> Eun Ae Kim,<sup>†</sup> Yun Ju Kim,<sup>†</sup> Young-A Lee,<sup>‡</sup> Youngshang Pak,<sup>†</sup> and Ok-Sang Jung<sup>\*†</sup>

Department of Chemistry (BK21) and Center for Plastic Information System, Pusan National University, Pusan 609-735, and Department of Chemistry, Chonbuk National University, Jeonju 561-756, Korea

Received October 19, 2004

Studies of the anion effects on the molecular construction of a series of AgX complexes with bis(4-pyridyl)-dimethylsilane (L) ( $X^- = \text{NO}_2^-, \text{NO}_3^-, \text{CF}_3\text{SO}_3^-, \text{and PF}_6^-$ ) have been carried out. Formation of the skeletal bonds appears to be primarily associated with a suitable combination of bidentate N-donors of L and a variety of coordination geometries of Ag(I) ions. The L:Ag(I) ratios of the products are dependent on the nature of the polyatomic anions. The 1:1 adduct Ag(I)–L for  $\text{NO}_2^-$ , 3:4 adduct for  $\text{NO}_3^-$ , 2:3 adduct for  $\text{CF}_3\text{SO}_3^-$ , and 1:2 adduct for  $\text{PF}_6^-$  have been obtained. A linear relationship between the ratio of ligand to metal and the coordinating ability of anions was observed.  $[\text{Ag}(\text{NO}_2)(\text{L})]$  has a unique sheet structure consisting of double helices, and  $[\text{Ag}_3(\text{L})_4](\text{NO}_3)_3$  is a 2 nm thick interwoven sheet structure consisting of nanotubes. The compound  $[\text{Ag}_2(\text{L})_3](\text{CF}_3\text{SO}_3)_2$  affords a characteristic ladder-type channel structure, and  $[\text{Ag}(\text{L})_2](\text{PF}_6)$  is a simple 2D grid structure.

### Introduction

The rational design and construction of functional coordination materials with specific motifs is a fruitful field since the materials have various potential applications such as molecular separation, toxic materials adsorption, molecular containers, ion exchangers, molecular recognition, and luminescent sensors.<sup>1–6</sup> Thus, various kinds of framework materials have been constructed by the coordinations of metal ions with spacer ligands.<sup>7–18</sup> The molecular geometry and

flexibility of multidentate N-donor spacer ligands play key roles in the development of the tailor-made molecular materials. Recently, we have demonstrated that various silicon-containing pyridyl spacer ligands are useful for the synthesis of desirable skeletal structures.<sup>19–23</sup> Exploitation of the silicon-containing pyridine-based ligands has produced a variety of coordination modes since the ligands are adjustable in their potential bridging ability, possess flexible interligand angles at silicon, and are conformationally nonrigid. Furthermore, the counteranions can play crucial roles in the molecular construction since the anions have many features such as negative charge, size, and geometry, and display variable differences, significant solvent effects,

\* Author to whom correspondence should be addressed. E-mail: oksjung@pusan.ac.kr.

<sup>†</sup> Pusan National University.

<sup>‡</sup> Chonbuk National University.

- (1) Stang, P. J.; Olenyuk, B. *Acc. Chem. Res.* **1997**, *30*, 502.
- (2) Jones, C. J. *Chem. Soc. Rev.* **1998**, *27*, 289.
- (3) Slone, R. V.; Yoon, D. I.; Calhoun, R. M.; Hupp, J. T. *J. Am. Chem. Soc.* **1995**, *117*, 11813.
- (4) Gale, P. A. *Coord. Chem. Rev.* **2001**, *213*, 79–128.
- (5) Fujita, M. *Chem. Soc. Rev.* **1998**, *27*, 417.
- (6) Jung, O.-S.; Kim, Y. J.; Lee, Y.-A.; Park, J. K.; Chae, H. K. *J. Am. Chem. Soc.* **2000**, *122*, 9921.
- (7) Albrecht, M. *Angew. Chem., Int. Ed.* **1999**, *38*, 3463.
- (8) Jones, C. J. *Chem. Soc. Rev.* **1998**, *27*, 289.
- (9) Batten, S. R.; Robson, R. *Angew. Chem., Int. Ed.* **1998**, *37*, 1460.
- (10) Constable, E. C. *Tetrahedron* **1992**, *48*, 10013.
- (11) Chui, S. S.-Y.; Lo, S. M.-F.; Charmant, J. P. H.; Orpen, A. G.; Williams, I. D. *Science* **1999**, *283*, 1148.
- (12) Kiang, Y.-H.; Gardener, G. B.; Lee, S.; Xu, Z. *J. Am. Chem. Soc.* **2000**, *122*, 6871.
- (13) Braga, D.; Grepioni, F. *Acc. Chem. Res.* **2000**, *33*, 601.
- (14) Schmidtchen, F. P.; Berger, M. *Chem. Rev.* **1997**, *97*, 1609.

- (15) Lapointe, R. E.; Roof, G. R.; Abboud, K. A.; Klosin, J. *J. Am. Chem. Soc.* **2000**, *122*, 9560.
- (16) Mason, S.; Clifford, T.; Seib, L.; Kuczera, K.; Bowman-James, K. *J. Am. Chem. Soc.* **1998**, *120*, 8899.
- (17) Jung, O.-S.; Kim, Y. J.; Lee, Y.-A.; Chae, H. K.; Jang, H. G.; Hong, J. K. *Inorg. Chem.* **2001**, *40*, 2105.
- (18) Jung, O.-S.; Park, S. H.; Kim, K. M.; Jang, H. G. *Inorg. Chem.* **1998**, *37*, 5781.
- (19) Jung, O.-S.; Kim, Y. J.; Kim, K. M.; Lee, Y.-A. *J. Am. Chem. Soc.* **2002**, *124*, 7906.
- (20) Lee, Y.-A.; Kim, S. A.; Jung, S. M.; Jung, O.-S.; Oh, Y. H. *Bull. Korean Chem. Soc.* **2004**, *25*, 581.
- (21) Jung, O.-S.; Lee, Y.-A.; Kim, Y. J. *Chem. Lett.* **2002**, 1096.
- (22) Jung, O.-S.; Lee, Y.-A.; Kim, Y. J.; Hong, J. *Cryst. Growth Des.* **2002**, *2*, 497.
- (23) Jung, O.-S.; Kim, Y. J.; Lee, Y.-A.; Kang, S. W.; Choi, S. N. *Cryst. Growth Des.* **2004**, *4*, 23.

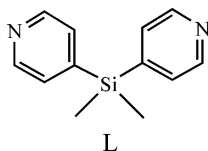
**Table 1.** Crystallographic Data

	[Ag(NO <sub>2</sub> )(L)]	[Ag <sub>2</sub> (L) <sub>3</sub> ](CF <sub>3</sub> SO <sub>3</sub> ) <sub>2</sub> ·2CH <sub>3</sub> OH	[Ag(L) <sub>2</sub> ](PF <sub>6</sub> ) <sup>1/2</sup> ·CH <sub>3</sub> C(O)CH <sub>3</sub>
empirical formula	C <sub>12</sub> H <sub>14</sub> N <sub>3</sub> O <sub>2</sub> SiAg	C <sub>19</sub> H <sub>21</sub> N <sub>3</sub> O <sub>3</sub> F <sub>3</sub> SSi <sub>1.5</sub> S <sub>2</sub> Ag·2CH <sub>3</sub> OH <sub>1</sub>	C <sub>48</sub> H <sub>56</sub> N <sub>8</sub> F <sub>12</sub> N <sub>8</sub> P <sub>2</sub> Si <sub>4</sub> Ag <sub>2</sub> ·CH <sub>3</sub> C(O)CH <sub>3</sub>
fw	368.22	610.50	1421.13
space group	C2/c	C2/c	P1
a, Å	24.557(3)	22.117(6)	11.1074(8)
b, Å	9.649(2)	12.714(3)	16.540(1)
c, Å	13.906(2)	21.976(6)	18.666(1)
α, deg			77.082(1)
β, deg	115.63(2)	99.218(5)	80.911(1)
γ, deg			76.968(1)
V, Å <sup>3</sup>	2970.8(8)	6100(3)	3235.3(4)
Z	8	8	2
d <sub>calcd</sub> , gcm <sup>-3</sup>	1.647	1.330	1.459
μ, mm <sup>-1</sup>	1.438	0.832	0.804
R {I > 2σ(I)}	R1 <sup>a</sup> = 0.0722 wR2 <sup>b</sup> = 0.22.86	R1 = 0.0754 wR2 = 0.1936	R1 = 0.0537 wR2 = 0.1260
R (all data)	R1 = 0.0729 wR2 = 0.2301	R1 = 0.2805 wR2 = 0.2832	R1 = 0.1727 wR2 = 0.1834

$$^a R1 = \sum ||F_o| - |F_c|| / \sum |F_o|. \quad ^b wR2 = \sum w(F_o^2 - F_c^2)^2 / \sum wF_o^2)^{1/2}.$$

and pH dependence.<sup>4,24–27</sup> Recent developments in anion chemistry include exciting advances in anion template assembly, ion-pair recognition, and the function of supramolecular materials.<sup>28–31</sup>

In an effort to expand the roles of anions in the molecular construction, the slow diffusion reactions of AgX (X<sup>-</sup> = NO<sub>2</sub><sup>-</sup>, NO<sub>3</sub><sup>-</sup>, CF<sub>3</sub>SO<sub>3</sub><sup>-</sup>, and PF<sub>6</sub><sup>-</sup>) with bis(4-pyridyl)-dimethylsilane (L) were carried out and scrutinized. The Ag(I) ion has been employed as various directional units such as linear, T-shaped, and tetrahedral geometry.<sup>32</sup>



## Experimental Section

**Materials and Measurements.** AgX (X<sup>-</sup> = NO<sub>2</sub><sup>-</sup>, NO<sub>3</sub><sup>-</sup>, CF<sub>3</sub>SO<sub>3</sub><sup>-</sup>, and PF<sub>6</sub><sup>-</sup>) were purchased from Strem, and were used without further purification. Bis(4-pyridyl)dimethylsilane (L) was prepared according to the literature procedure.<sup>33</sup> [Ag<sub>3</sub>(L)<sub>4</sub>](NO<sub>3</sub>)<sub>3</sub> was recently published as a Communication.<sup>19</sup> Elemental microanalyses (C, H, N) were performed on crystalline samples by the Advanced Analysis Center at KIST using a Perkin-Elmer 2400 CHN analyzer. X-ray powder diffraction data were recorded on a Rigaku RINT/DMAX-2500 diffractometer at 40 kV and 126 mA for Cu Kα. Thermal analyses were carried out under a dinitrogen atmosphere at a scan rate of 10 °C/min using a Stanton Red Croft TG 100. Infrared spectra were obtained on a Perkin-Elmer 16F PC FTIR spectrophotometer with samples prepared as KBr pellets.

**[Ag(NO<sub>2</sub>)(L)].** A methanol solution (6 mL) of L (43 mg, 0.20 mmol) was slowly diffused into an aqueous solution (6 mL) of AgNO<sub>2</sub> (30 mg, 0.20 mmol). Colorless crystals of [Ag(NO<sub>2</sub>)(L)] formed at the interface, and were obtained in 6 days in 70% yield. Mp: 164 °C dec. Anal. Calcd for C<sub>12</sub>H<sub>14</sub>N<sub>3</sub>O<sub>2</sub>SiAg: C, 39.14; H, 3.83; N, 11.41. Found: C, 40.04; H, 3.77; N, 11.14. IR (KBr, cm<sup>-1</sup>): ν(NO<sub>2</sub>), 1254 (s).

**[Ag<sub>2</sub>(L)<sub>3</sub>](CF<sub>3</sub>SO<sub>3</sub>)<sub>2</sub>.** A methanol solution of L was slowly diffused into an aqueous solution of AgCF<sub>3</sub>SO<sub>3</sub> in a mole ratio of 1:1. Yield: 70% based on Ag(I) salt. Mp: 252 °C dec. Anal. Calcd for C<sub>38</sub>H<sub>42</sub>N<sub>6</sub>O<sub>6</sub>F<sub>6</sub>S<sub>2</sub>Si<sub>3</sub>Ag<sub>2</sub>: C, 39.45; H, 3.66; N, 7.26. Found: C, 40.01; H, 3.76; N, 7.24. The crystals were obtained as a methanol

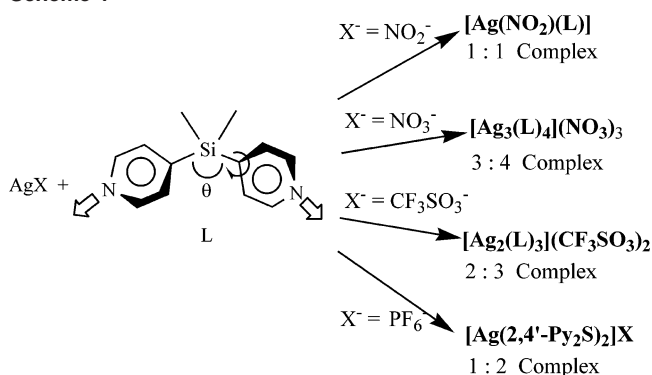
solvate, but the elemental analysis was accomplished after desolvation under vacuum. IR (KBr, cm<sup>-1</sup>): ν(CF<sub>3</sub>SO<sub>3</sub>), 814 (s).

**[Ag(L)<sub>2</sub>](PF<sub>6</sub>).** This reaction was carried out by a similar method using acetone instead of methanol as a solvent. Yield: 70%. Mp: 210 °C dec. Anal. Calcd for C<sub>24</sub>H<sub>28</sub>N<sub>4</sub>PF<sub>6</sub>Si<sub>2</sub>Ag: C, 42.40; H, 4.14; N, 8.22. Found: C, 42.30; H, 4.18; N, 8.48. IR (KBr, cm<sup>-1</sup>): ν-(PF<sub>6</sub>), 838 (s). The crystals were obtained as an acetone solvate, but the elemental analysis was accomplished after desolvation under vacuum.

**Crystallographic Structure Determinations.** X-ray data were collected on a Bruker SMART automatic diffractometer with graphite-monochromated Mo Kα radiation (λ = 0.71073 Å) and a CCD detector at ambient temperature. The 45 frames of two-dimensional diffraction images were collected and processed to obtain the cell parameters and orientation matrix. The data were corrected for Lorentz and polarization effects. Absorption effects were corrected by the empirical ψ-scan method. The structures were solved by the direct method (SHELXS 97) and refined by full-matrix least-squares techniques (SHELXL 97).<sup>34</sup> The non-hydrogen atoms were refined anisotropically, and hydrogen atoms were placed in calculated positions and refined only for the isotropic thermal factors. Crystal parameters and procedural information corresponding to data collection and structure refinement are given in Table 1.

- (24) Jung, O.-S.; Kim, Y. J.; Lee, Y.-A.; Park, K.-M.; Lee, S. S. *Inorg. Chem.* **2003**, *42*, 844.
- (25) Withersby, M. A.; Blake, A. J.; Champness, N. R.; Hubberstey, P.; Li, W.-S.; Schröder, M. *Angew. Chem., Int. Ed. Engl.* **1997**, *36*, 2327.
- (26) Wu, H. P.; Janiak, C.; Rheinwald, G.; Lang, H. *J. Chem. Soc., Dalton Trans.* **1999**, 183–190.
- (27) Janiak, C.; Uehlin, L.; Wu, H.-P.; Klufers, P.; Piotrowski, H.; Scharmann, T. G. *J. Chem. Soc., Dalton Trans.* **1999**, 3121.
- (28) Reed, C. A. *Acc. Chem. Res.* **1998**, *31*, 133.
- (29) Campos-Fernandez, C. S.; Clerac, R.; Dunbar, K. R. *Angew. Chem., Int. Ed.* **1999**, *38*, 3477.
- (30) Turner, B.; Shterenberg, A.; Kapon, M.; Suwinska, K.; Eichen, Y. *Chem. Commun.* **2001**, 13.
- (31) Sharma, C. V. K.; Griffin, S. T.; Rogers, R. D. *Chem. Commun.* **1998**, 215.
- (32) Munakata, M.; Wu, L. P.; Kuroda-Sowa, T. *Adv. Inorg. Chem.* **1999**, *46*, 173.
- (33) Schmitz, M.; Leninger, S.; Fan, J.; Arif, A. M.; Stang, P. J. *Organometallics* **1999**, *18*, 4817.
- (34) Sheldrick, G. M. SHELXS-97: A Program for Structure Determination, University of Göttingen, Germany, 1997. Sheldrick, G. M. SHELXL-97: A Program for Structure Refinement, University of Göttingen, Germany, 1997.

Scheme 1



## Results and Discussion

**Synthesis.** The slow diffusion of an organic solution of bis(4-pyridyl)dimethylsilane (L) into an aqueous solution of  $\text{AgX}$  ( $X^- = \text{NO}_2^-$ ,  $\text{NO}_3^-$ ,  $\text{CF}_3\text{SO}_3^-$ , and  $\text{PF}_6^-$ ) afforded the 1:1  $\text{Ag}(\text{I})\text{-L}$  adduct for  $\text{NO}_2^-$ , 3:4 adduct for  $\text{NO}_3^-$ ,<sup>19</sup> 2:3 adduct for  $\text{CF}_3\text{SO}_3^-$ , and 1:2 adduct for  $\text{PF}_6^-$ , presumably owing to the different coordinating natures of the anions (Scheme 1). The ratios are exactly coincident with the order of coordinating ability of the anions as established in our previous results.<sup>24</sup> The slow diffusion reactions were originally conducted at a 1:1 mole ratio of  $\text{Ag}(\text{I})$  and L, but the products were not significantly affected by the mole ratio. Moreover, when acetone or ethanol was used as solvent instead of methanol, the same products were obtained. That is, the assembled structures were dependent only on the anions. The reaction of  $\text{AgNO}_2$  with L produces a unique sheet structure consisting of double helices, whereas the treatment of  $\text{AgPF}_6$  with L gives a simple network structure.  $[\text{Ag}_3(\text{L})_4](\text{NO}_3)_3$  was a 2 nm thick interwoven sheet structure consisting of nanotubes.<sup>19</sup> The reaction of  $\text{AgCF}_3\text{SO}_3$  with L affords a unique 1D ladder channel structure. All the crystalline products are insoluble in water and common organic solvents, and are stable for several days even in aqueous suspensions.

**Structures.** The crystal structure of  $[\text{Ag}(\text{NO}_2)(\text{L})]$  is shown in Figure 1, and relevant structural data are listed in Table 2. Each L connects two  $\text{Ag}(\text{I})$  ions ( $\text{Ag}-\text{N} = 2.231(8)$  and  $2.240(8)$  Å) to form a helix (helical pitch  $19.298(2)$  Å). Each single helix twists the adjacent helix (phase difference  $9.649(2)$  Å) to form an elegant double helix that is comparable to the structure of  $[\text{Ag}(\text{bpp})](\text{CF}_3\text{SO}_3)$ .<sup>35</sup> The formation of helical molecules may be attributed to a favorable combination of the skewed conformer of L and the appropriate geometry around the  $\text{N}-\text{Ag}-\text{N}$  bonds. The nitrite anion is chelated to the  $\text{Ag}(\text{I})$  ion ( $\text{Ag}-\text{O}(1) = 2.43(1)$  Å,  $\text{Ag}-\text{O}(2) = 2.51(1)$  Å). The angle  $\text{N}(1)-\text{Ag}-\text{N}(2)$  ( $126.9(3)^\circ$ ) indicates that the nitrite acts as a bidentate ligand rather than a simple counteranion. The double helices are connected to each other via the  $\text{Ag}\cdots\text{Ag}$  interactions ( $3.002(2)$  Å) to form a unique sheet. The unique sheet is similar to

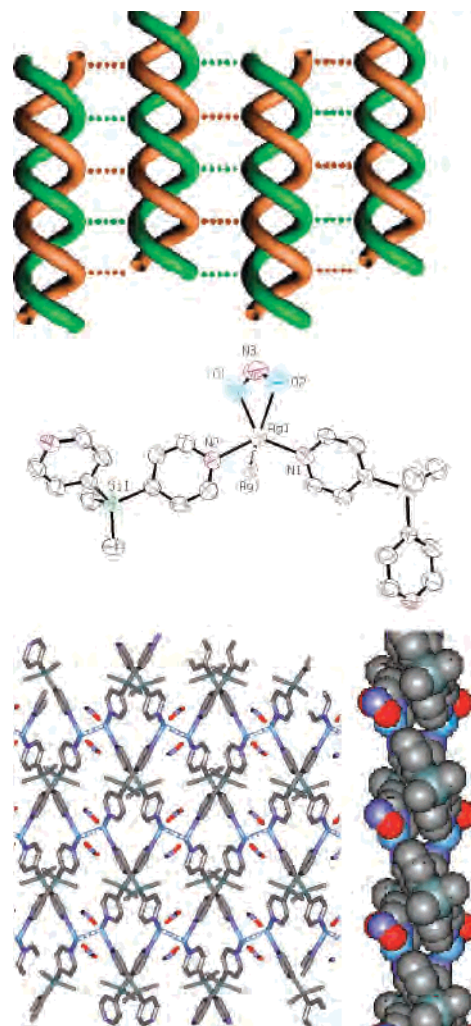


**Figure 1.** Schematic diagram (top), geometry around silver(I) (middle), and infinite structure (bottom) of  $[\text{Ag}(\text{NO}_2)(\text{L})]$ . Hydrogen atoms were omitted for clarity.

that of  $[\text{Ag}(2,4'\text{-bpy})](\text{ClO}_4)$ .<sup>36</sup> The interaction distance is similar to the known closed-shell  $d^{10}$   $\text{Ag}\cdots\text{Ag}$  interactions.<sup>37</sup> The argentophilic interaction is shorter than the van der Waals radii ( $3.44$  Å), and is rather close to the  $\text{Ag}-\text{Ag}$  distance in silver metal ( $2.89$  Å).<sup>38</sup> That is, the  $\text{Ag}(\text{I})$  ion may be best described as five-coordinate. Even though the nitrite acts as a bidentate, the central  $\text{Ag}(\text{I})$  ion has a five-coordination number including an argentophilic  $\text{Ag}\cdots\text{Ag}$  interaction, which will be explained in detail.

The molecular structure of  $[\text{Ag}_2(\text{L})_3](\text{CF}_3\text{SO}_3)_2 \cdot 2\text{CH}_3\text{OH}$  is depicted in Figure 2, and selected data are listed in Table 2. Its skeleton is a ladder structure consisting of a 2:3 ratio of  $\text{Ag}(\text{I})$  and L. Three pyridyl moieties connect a  $\text{Ag}(\text{I})$  ion ( $\text{Ag}-\text{N} = 2.248(7)$ ,  $2.244(1)$ , and  $2.311(8)$  Å) to form a ladder structure. Thus, the geometry around the  $\text{Ag}(\text{I})$  ion approximates a trigonal arrangement ( $\text{N}-\text{Ag}-\text{N} = 115.8(3)$ – $122.0(3)^\circ$ ). The most fascinating feature is that the top view of the molecular ladder is an elegant tubular structure.

(36) Tong, M.-L.; Chen, X.-M.; Ye, B.-H.; Ng, S. W. *Inorg. Chem.* **1998**, *37*, 5278.

(37) Tong, M.-L.; Chen, X.-M.; Ye, B.-H.; Ji, L.-N. *Angew. Chem., Int. Ed.* **1999**, *38*, 2237.

(38) Wang, Q.-M.; Mak, T. C. W. *J. Am. Chem. Soc.* **2000**, *122*, 7608.

(35) Carlucci, L.; Ciani, G.; Gudenberg, D. W. V.; Proserpio, D. M. *Inorg. Chem.* **1997**, *36*, 3812.

**Table 2.** Selected Bond Parameters and Structural Features

	[Ag(NO <sub>2</sub> )(L)]	[Ag <sub>3</sub> (L) <sub>4</sub> ](NO <sub>3</sub> ) <sub>3</sub> <sup>a</sup>	[Ag <sub>2</sub> (L) <sub>3</sub> ](CF <sub>3</sub> SO <sub>3</sub> ) <sub>2</sub> · 2CH <sub>3</sub> OH	[Ag(L) <sub>2</sub> ](PF <sub>6</sub> ) · 1/2CH <sub>3</sub> C(O)CH <sub>3</sub>
Ag–N (Å)	2.231(8), 2.240(8)	2.14(1)–2.34(1)	2.244(7)–2.311(8)	2.266(5)–2.419(5)
N–Ag–N (deg)	126.9(3)	160.1(6)	115.8(3)–122.0(3)	100.2(2)–114.1(2)
Py–Si–Py (deg)	107.6(4)	105.9(7)–109.7(7)	108.3(4), 107.4(5)	104.8(3)–107.9(3)
Ag···X (Å)	2.43(1), 2.51(1)	2.51(4)	2.882(3)	> 3.00
coord number	5	2, 3	3	4
motif	double helix	interwoven nanotube	ladder tube	network

<sup>a</sup> Reference 19.

The molecular tube has a 14 Å × 12 Å cross section. The triflate anion does not significantly interact with the Ag(I) ion and, thus, acts as a simple counteranion (Ag···O = 2.882–(3) Å).

For the PF<sub>6</sub><sup>−</sup> analogue, the skeletal structure is simple networks consisting of a 1:2 mole ratio of Ag and L. The crystal structure is shown in Figure 3, and selected bond lengths and angles are listed in Table 2. Each L connects two Ag(I) ions (Ag–N = 2.266(5)–2.419(5) Å) to form a [Ag(L)<sub>2</sub>]<sub>4</sub> rectangle (11 Å × 11 Å) motif. For the network structure, the geometry around the Ag(I) is a distorted tetrahedral arrangement (N–Ag–N = 96.7(2)–124.8(2)°). The PF<sub>6</sub><sup>−</sup> anion exist as a simple counteranion. The crystal is composed of abab... layers.

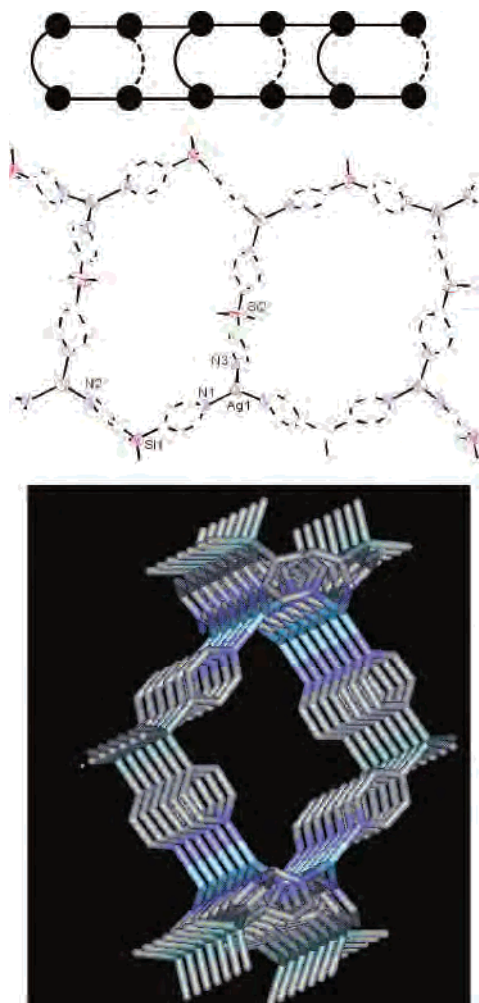


**Figure 2.** Schematic diagram (top), geometry around silver(I) (middle), and infinite structure (bottom) of [Ag<sub>2</sub>(L)<sub>3</sub>](CF<sub>3</sub>SO<sub>3</sub>)<sub>2</sub>. Hydrogen and triflate anions were omitted for clarity.

**Construction Principle.** A combination of a variety of geometries of Ag(I) ions and the appropriate length, conformation, angle, and steric effects of the L ligand seems to afford characteristic structures with various ratios of L to Ag(I). Each skeleton was exclusively constructed irrespective of the mole ratio of the reactants, the solvent types, and the concentrations. The Ag(I):L ratios of the products (1:1, 3:4, 2:3, and 1:2) are dependent on the anions. First of all, the PF<sub>6</sub><sup>−</sup> anion that has been considered as a common “noncoordinating” anion<sup>39</sup> has little tendency to serve as a ligand

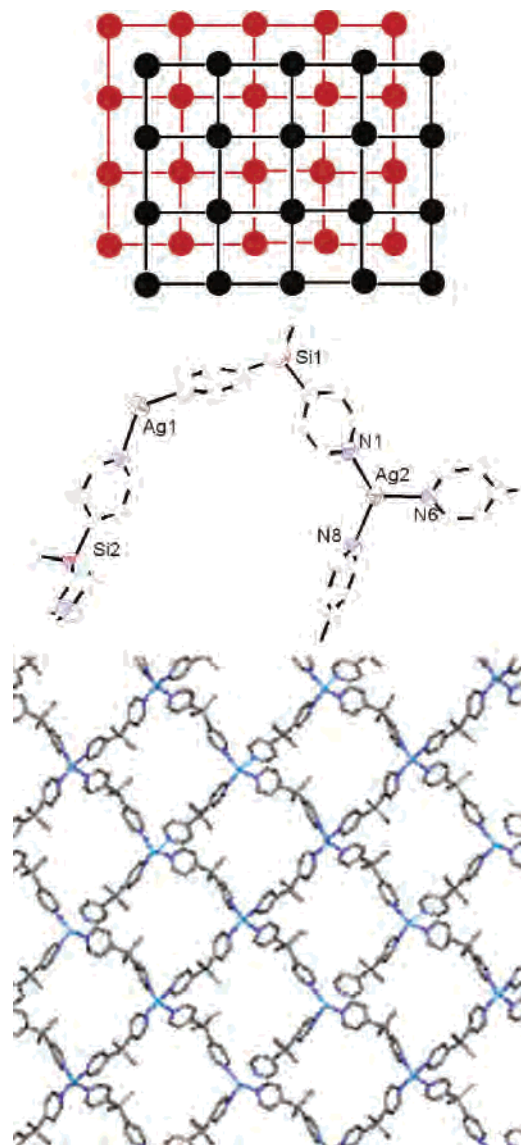


**Figure 3.** Schematic diagram (top), geometry around silver(I) (top), and infinite structure (bottom) of [Ag(L)<sub>2</sub>](PF<sub>6</sub>). Hydrogen and hexafluorophosphate anions were omitted for clarity.

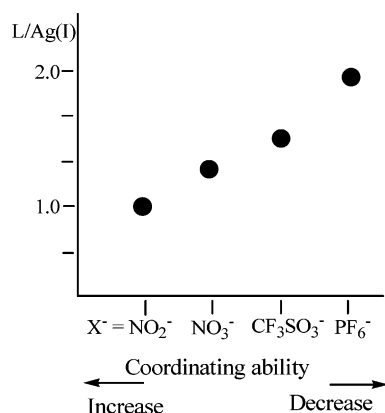


**Figure 4.** Correlation between the L:Ag(I) ratio and the coordination ability of the anions.

in the present structure. Such noncoordinating anions afford the spacer-abundant 1:2 adducts of  $[\text{Ag}(\text{L})_2](\text{PF}_6)$ . On the other hand, a relatively coordinating anion,  $\text{NO}_2^-$ ,<sup>40</sup> affords the 1:1 adduct of  $[\text{Ag}(\text{NO}_2)(\text{L})]$ . The moderately coordinating  $\text{NO}_3^-$  anion produces  $[\text{Ag}_3(\text{L})_4](\text{NO}_3)_3$  (3:4). Triflate anion affords the 2:3 adduct of  $[\text{Ag}_2(\text{L})_3](\text{CF}_3\text{SO}_3)_2$ . The ratios are exactly coincident with the order of the coordinating ability of the anions that was established in our previous paper.<sup>24</sup>

For  $[\text{Ag}(\text{NO}_2)(\text{L})]$ , the  $\text{NO}_2^-$  anion acts as a chelate ligand rather than a simple counteranion. The bond length of Ag–O is 2.43(1) and 2.51(1) Å, and thus, the bond angle of N–Ag–N (126.9(3)°) is concomitantly bent. Furthermore, the coordinating  $\text{NO}_2^-$  moiety partly seems to induce a double-helical motif. The double helices are connected to each other via the  $\text{Ag}\cdots\text{Ag}$  interaction (3.002(2) Å) to form a characteristic molecular sheet. For  $[\text{Ag}_3(\text{L})_4](\text{NO}_3)_3$  and  $[\text{Ag}_2(\text{L})_3](\text{CF}_3\text{SO}_3)_2$ , the shortest  $\text{Ag}\cdots\text{NO}_3^-$  (2.51 Å)<sup>19</sup> and  $\text{Ag}(\text{I})\cdots\text{CF}_3\text{SO}_3^-$  (2.88 Å) distances are less than the sum of the van der Waals radii (3.20 Å) of Ag and O.<sup>41</sup> The L/M ratios as well as the local geometries of the products appear to be delicately associated with the coordinating nature of the anions. The L/M ratios increase with decreasing order

of coordinating ability,  $\text{NO}_2^- < \text{NO}_3^- < \text{CF}_3\text{SO}_3^- < \text{PF}_6^-$ , as shown in Figure 4. For the products with noncoordinating anions, no  $\pi$ – $\pi$  interaction exists, in contrast to 2,4'-Py<sub>2</sub>S analogues,<sup>24</sup> presumably owing to the presence of the bulky dimethyl groups. The bond angles of Py–Si–Py (104.8(1)–108.2(1)°) are almost constant, indicating that the present ligand is relatively rigid.

**Thermal Properties.** All crystals are insoluble in water and common organic solvents. The products are air-stable, but slowly turn to gray powder under light. The crystalline solids are easily dissociated in dimethyl sulfoxide, *N,N*-dimethylformamide, or acetonitrile. The thermal stabilities are dependent upon the structural properties. For  $[\text{Ag}(\text{NO}_2)(\text{L})]$ , the thermal analyses (TGA and DSC) (Supporting Information) show a drastic decomposition around 164 °C. The collapse at low temperature relative to that of  $[\text{Ag}_3(\text{L})_4](\text{NO}_3)_3$  (231 °C)<sup>19</sup> may be ascribed to the angle constraint of the chelating  $\text{NO}_2^-$  moiety and the inter-double-helical argentophilic interaction.  $[\text{Ag}(\text{L})_2](\text{PF}_6)$  is stable up to 210 °C. The TGA and DSC overlay of  $[\text{Ag}_2(\text{L})_3](\text{CF}_3\text{SO}_3)_2$  indicates that the tubular structure is stable up to 252 °C, indicating that the tube structure is more or less rigid.

In conclusion, our results demonstrate that the silicon-based bipyridine spacer is a fascinating molecular building unit that exhibits little strain in the construction of various skeletons such as a double-helical sheet with a ligand-unsupported  $\text{Ag}\cdots\text{Ag}$  interaction in five-coordinate Ag(I) compounds, a sheet consisting of nanotubes, ladder type tubes, and 2D sheets. In particular, the L/M ratios of the products are strongly dependent upon the coordinating order of the anions. A new coordinating series of polyatomic anions may be used to quantitatively predict and synthesize the desired structures.

**Acknowledgment.** This work was supported financially by Grant KRF-2003-015-C00308 in Korea.

**Supporting Information Available:** Crystallographic data for  $[\text{Ag}(\text{NO}_2)(\text{L})]$ ,  $[\text{Ag}_2(\text{L})_3](\text{CF}_3\text{SO}_3)_2$ , and  $[\text{Ag}(\text{L})_2](\text{PF}_6)$  (CIF) and TGA and DSC data (PDF). This information is available free of charge via the Internet at <http://pubs.acs.org>.

IC048537R

(39) Chew, K. F.; Healy, M. A.; Khalil, M. I.; Logan, N.; Derbyshire, W. *J. Chem. Soc., Dalton Trans.* **1975**, 1315.

(40) Jung, O.-S.; Kim, Y. J.; Park, J. Y.; Choi, S. N. *J. Mol. Struct.* **2003**, *657*, 207.

(41) Huheey, J. E. *Inorganic Chemistry, Principles of Structure and Reactivity*, 2nd ed.; Harper & Row: New York, 1978; pp 230.